Colloid Polym Sci 279:947–958 (2001)

ORIGINAL CONTRIBUTION

J.-L. Luna-Xavier
E. Bourgeat-Lami
A. Guyot

The role of initiation in the synthesis of silica/poly(methyl methacrylate) nanocomposite latex particles through emulsion polymerization

Received: 8 December 2000
Accepted: 22 February 2001

J.-L. Luna-Xavier
E. Bourgeat-Lami (✉) · A. Guyot
LCPP/CNRS-CPE – Bât 308F
43 Boulevard du 11 Novembre 1918
BP 2077, 69616 Villeurbanne Cedex
France

Abstract Silica/poly(methyl methacrylate) nanocomposite latex particles have been synthesized by emulsion polymerization of methyl methacrylate using a nonionic surfactant: nonylphenol poly(oxyethylene) and three different initiators, namely: 2,2′-azobis(2-amidinopropane) dihydrochloride (AIBA), potassium persulfate (KPS) and azobis(isobutyronitrile) (AIBN), being cationic, anionic and nonionic, respectively. A silica sol with an average diameter of 68 nm was used as the seed. The polymerization reaction was conducted under alkaline conditions in order to evaluate the role of the surface charge of the hydrophilic silica on the coating reaction. AIBA was found to be adsorbed on the silica surface owing to electrostatic interactions of the amidine function of the cationic initiator with the silanolate groups of the oxide surface, while the anionic and the nonionic initiators did not adsorb on silica under the same conditions. Nonetheless, whatever the nature of the initiator, polymerization took place on the silica particles as evidenced by transmission electron microscopy. The extent of interaction between the inorganic surface and the polymer particles was quantified by means of ultracentrifugation and a material balance. As much as 65% by weight of the total polymer formed was found to be present at the silica surface using AIBA, while only 40% for KPS and 25% for AIBN was found to cover the silica particles under alkaline conditions. We demonstrate that by using a cationic initiator and by controlling the pH of the suspension it is possible to significantly decrease the amount of free polymer. Coating of the silica particles took place through a kind of in situ heterocoagulation mechanism.

Key words Emulsion polymerization · Heterocoagulation · Coating · Silica · Nanocomposite particles

Introduction

In recent years, a great number of scientists have dedicated their efforts to the elaboration of new composite systems. Very interesting applications of multiphase materials can be found in the biomedical field [1, 2], in optic [3], microelectronic and automotive industries. Among the large number of strategies which have been developed for the synthesis of multiphase systems, microencapsulation technologies provide a variety of methods which are largely used in agriculture, food and pharmaceutical areas, for instance. A particular category of encapsulated materials are fillers and pigments. The encapsulation reactions of fillers and pigments have been reviewed recently by van Herk and German [4]. Although a lot of procedures exist, emulsion polymerization is by far the technique most frequently used for the encapsulation reaction of minerals with polymers [4–8]. One

difficulty, however, of encapsulation reactions through emulsion polymerization resides in the fact that inorganic surfaces are hydrophilic, while polymers are hydrophobic. In order to promote polymerization on the inorganic surface, modification of the mineral can be carried out by using, for instance, silane or titanate molecules reactive in free radical polymerization [9–11]. The adsorption of bilayers forming surfactants has also been widely studied and provides hydrophobic loci for the solubilization of monomers and/or oligoradicals and their subsequent polymerization through a kind of (ad)micellar nucleation mechanism [12]. As an alternative, heterocoagulation, which involves the precipitation of preformed latex particles on the inorganic core surface, can also be envisaged [13]. However, none of these techniques enables the complete avoidance of the formation of free polymer, which almost always competes with the coating reaction. In order to improve the coating efficiency and to achieve high polymer concentrations on the inorganic surface, the amount of free surfactant can be controlled and maintained at concentrations just below the apparent critical micellar concentration of the soap [14]. A minimum surface area of the seed particles is required and better results are obtained when the monomer is added under starved feed conditions [12, 15, 16]. Of course, the nature of the surfactant, the monomer and the initiator molecules is also critical. A lot is gained, for instance, in using initiators with strong interactions with the inorganic surface and more hydrophobic monomers. Cationic initiators, for example 2,2′-azobis(2-amidinopropane) dihydrochloride (AIBA), have been used for the encapsulation reaction of titanium dioxide pigments. A high amount of encapsulating polymer was obtained when the terminal ionic group of the polymer chain and the surface charge of the inorganic particles were oppositely charged [17]. AIBA has also been used in the polymerization reaction of vinyl monomers on several clays substrates [18]. It was demonstrated that AIBA was adsorbed on the mineral surface by means of an ion-exchange reaction [19]. In a related approach, AIBA was adsorbed on mica, a layered silicate, and the attached free radical was involved in the polymerization reaction of styrene [20]. Significant amounts of polymer grafted to the mineral surface were obtained. Surprisingly, however, only a few studies using AIBA and colloidal silica are reported in the literature. Yoshinaga et al. [21] have synthesized monodisperse poly(methyl methacrylate)/SiO_2 and polystyrene/SiO_2 composites in alcoholic solutions using dispersion polymerization. It was shown that polystyrene bonding on the inorganic surface took place through electrostatic interactions.

Here, we report results on the coating reaction of silica nanoparticles by emulsion polymerization of methyl methacrylate, using nonionic nonylphenol poly(oxyethylene) (NP_{30}) and AIBA as a cationic initiator. AIBA was compared to an anionic and a nonionic initiator: potassium persulfate (KPS) and azobis(isobutyronitrile) (AIBN), respectively. The composite particles were fully characterized using transmission electron microscopy (TEM), IR spectroscopy, thermogravimetric and elemental analyses. We were particularly interested in the morphology of the nanocomposite particles and in the efficiency of the coating reaction.

Experimental

Materials

Methyl methacrylate (from Aldrich) was purified by distillation under reduced pressure before use. The nonionic NP_{30} (Gerland) and the initiators AIBA (Kodak), KPS (Acros) and AIBN (Aldrich) were used as received. The hydrophilic silica sol (Klebosol 30N50, Clariant) was centrifuged at 16,000 rpm for 30 min before use (Beckman Avanti 30 ultracentrifuge) in order to separate the particles whose diameter is much lower than the mean diameter of the sol.

Characterization of the silica sol

The silica particles size and particles size distribution were determined by dynamic light scattering (DLS) and TEM. DLS measurements were performed using a Malvern Autosizer Lo-C instrument. For TEM experiments, a drop of a diluted dispersion was put on a carbon film supported by a copper grid and placed in the vacuum of a Philips CM10 electron microscope. The specific surface area was determined by nitrogen adsorption at 77 K using the Brunauer–Emmett–Teller method (ASAP 2010, Micromeritics). The electrophoretic mobility of the silica sol was determined using a laser electrophoresis zeta potential analyzer (Zetasizer III from Malvern instruments). The analyses were carried out at 20 °C and the zeta potential was an average of three measurements. The ionic strength was kept constant by dilution of the silica sol into a 0.001 mol/l sodium chloride solution. The pH of the suspension was controlled by adding 0.1 N standard aqueous solution of sodium hydroxide. The results are reported in Table 1.

Adsorption of initiators on the silica surface

The adsorption of AIBA, AIBN and KPS on the silica surface was performed at pH 9.8 by addition of a dilute solution of the initiator to the silica sol under a nitrogen atmosphere and gentle stirring. The silica dispersion containing the initiator was kept refrigerated at 5 °C overnight to equilibrate. The dispersion was next centrifuged and the concentration of KPS or AIBN in the supernatant was determined by carbon elemental analyses. AIBA concentrations were determined by UV analysis of the serum using a calibration curve. The amount of initiator adsorbed on the silica surface was determined by the difference between the total amount and the free amount of initiator.

Table 1 Characterization of the silica sol

	D_n (nm) (DLS)	D_n (nm) (TEM)	D_w/D_n (TEM)	S (m^2/g) (BET)	pH	Zeta potential (mV)
Klebosol 30N50	70	72	1.07	56	9.8	−31

Table 2 Polymerization recipes for the synthesis of the silica/poly(methyl methacrylate) (*PMMA*) composite latexes

Ingredients (g)		Samples		
		JL22	JL148	JL9
Deionized water	pH 9.8	100	100	100
Silica	SiO_2	1.16	1.2	1
Surfactant	NP_{30}	0.6	0.68	0.64
Monomer	Methyl methacrylate	1.1	0.98	1.1
Initiator	Potassium persulfate	0.012	–	–
	Azobis(isobutyronitrile)	–	0.014	–
	2,2′-Azobis(2-amidinopropane) dihydrochloride	–	–	0.014

Synthesis of the silica/PMMA nanocomposite latexes

The polymerizations were carried out in batch at 60 °C for up to 24 h under a nitrogen atmosphere. The 300-ml glass reactor fitted with a condenser was charged with silica, NP_{30} and deionized water. Degassing was carried out for several hours under gentle stirring before increasing the temperature to 60 °C. Then, the initiator dissolved in 10 ml deionized water and the monomer were added at once to start the polymerization. The recipes are reported in Table 2.

Characterization of the silica/PMMA nanocomposite latexes

The monomer to polymer conversions were determined gravimetrically by measuring the solid content after removal of water and residual monomer by evaporation. Particles size were determined by DLS, and TEM images were taken to characterize the morphology of the nanocomposite particles.

Fig. 1 Procedure developed for the characterization of the composite latexes and the determination of the efficiency of the coating reaction

Efficiency of the coating reaction and polymer content of the composite particles

The coating reactions gave rise to the formation of both nanocomposite particles, i.e., silica particles surrounded by PMMA, and independent (free) latex particles. In order to determine the efficiency of the coating reaction, which corresponds to the weight fraction of polymer on the inorganic surface, the free latex particles were separated from the nanocomposite particles using a series of centrifugations/redispersions in water as depicted in Fig. 1. In a typical analysis, the original latex dispersion containing the composite silica/PMMA particles, the emulsifier, NP_{30} and the free latex particles was centrifuged at 15,000 rpm for 30 min. The supernatant solution (denoted as the serum) was carefully separated from the residue. The settled composite particles were washed with deionized water under stirring and again separated from the serum by centrifugation. The operation was repeated until there was no more solid in the supernatant solution. The curves in Fig. 2 indicate that at least 6 cycles of centrifugations/redispersions in water were necessary to ensure the complete extraction of the free polymer particles from the residue. The residue containing the coated mineral was dried at 50 °C,

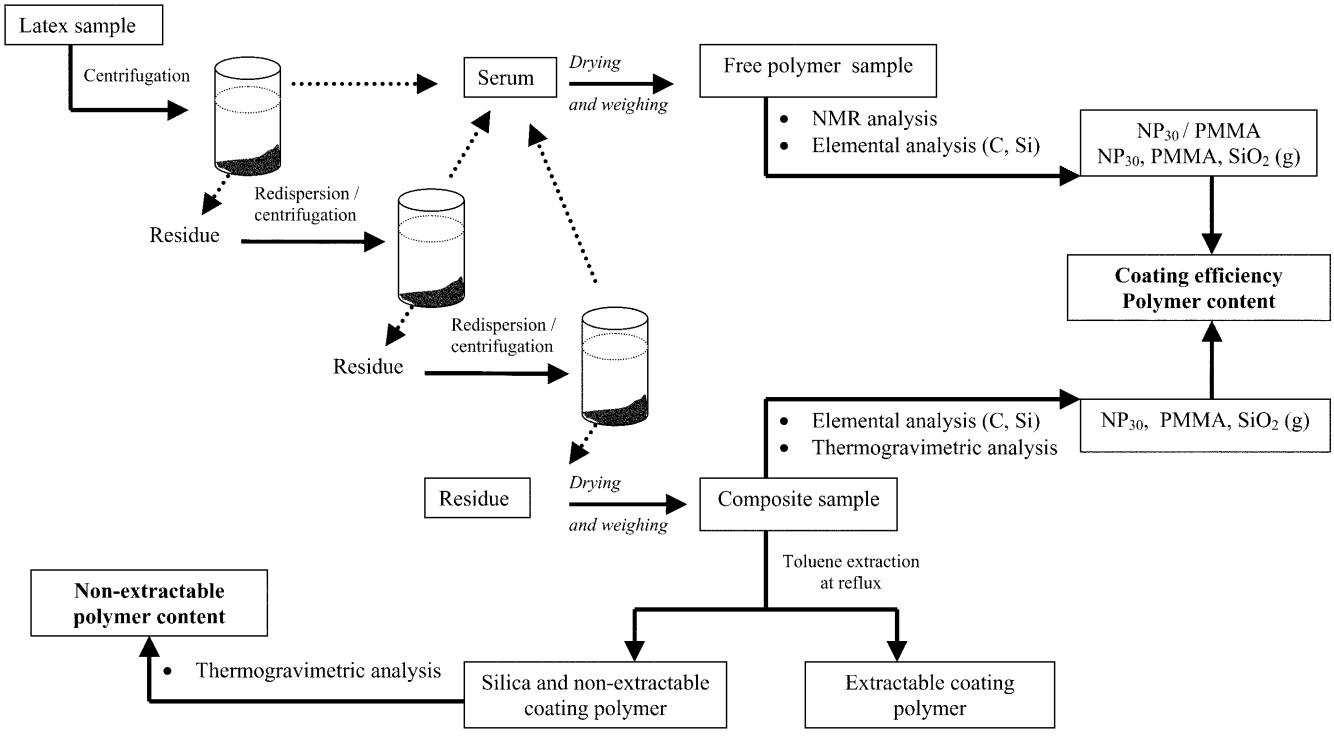

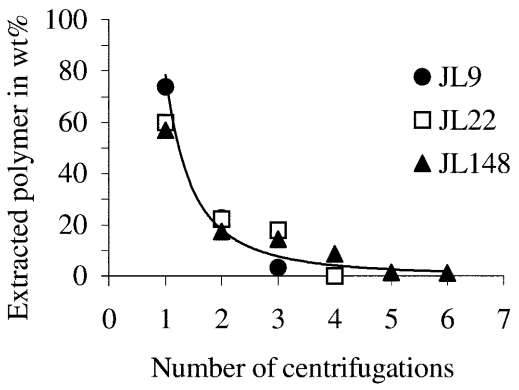

Fig. 2 Evolution of the weight fraction of extracted polymer (in grams per 100 g of the total amount of extractable polymer) which shows the number of centrifugation/redispersion cycles necessary to extract the totality of free polymer

weighted and analyzed by IR spectroscopy, thermogravimetric and elemental analyses. IR spectra were recorded using a Nicolet FTIR 460 spectrometer. Thermal analysis experiments were carried out using a thermogravimetric analyzer (TA 2950, Dupont Instruments) by heating the sample (10 mg) in a flow of helium (50 ml/min) at 10 °C/min from room temperature to 700 °C. The serum solutions containing the free polymer particles and the surfactant were collected separately into one solution and its solid content was determined gravimetrically. The composition of the serum was determined by elemental and ^{1}H NMR analyses. The ^{1}H NMR spectral analysis was carried out using a Brucker AC 250 MHz spectrometer with deuterated water. A mass balance was performed on silica, PMMA and NP_{30} to determine precisely the amount of each component in the different phases (i.e., the residue and the serum, respectively). The efficiency of the coating reaction and the polymer content were calculated as reported in Eqs. (1) and (2):

$$\text{Efficiency} = \frac{\text{amount of PMMA in the composite sample}}{\text{total amount of PMMA formed}} \times 100 \ , \quad (1)$$

Polymer content

$$= \frac{\text{amount of PMMA in the composite sample}}{\text{amount of composite sample}} \times 100 \ . \quad (2)$$

Nonextractable polymer content

After separation of the free polymer, the nanocomposite particles were suspended in hot toluene under reflux for 4 h to remove extractable polymer. The product after extraction was separated from the dissolved polymer by centrifugation and the weight fraction of nonextractable polymer was determined by thermogravimetric analysis of the recovered powder (Fig. 1). The nonextractable polymer content was calculated according to the following equation:

Nonextractable polymer content

$$= \frac{\text{amount of nonextractable polymer}}{\text{amount of recovered product after extraction}} \times 100 \ . \quad (3)$$

Polymer molecular weights and molecular weight distributions

In accordance with the procedure described previously, two distinct polymer fractions were isolated for analysis (Fig. 1): the free polymer and the extractable coating polymer.

The molecular weights and the molecular weight distributions of the free and the extractable coating polymers were determined by size-exclusion chromatography with a Waters 600 apparatus equipped with Shodex columns and a Waters R410 refractometer detector and using polystyrene standards.

Results

Initiators interaction with the silica surface

The results from elemental analysis indicate that the nonionic and the anionic initiators, AIBN and KPS, respectively, do not adsorb on the silica surface at high pH (Table 3). Indeed, attraction cannot take place under these conditions since AIBN does not carry any charges, while KPS and silica are of the same sign. Therefore, we prove that electrostatic repulsion forces between the negatively charged silica surface and the anionic initiator predominate at pH 9.8. In contrast, our results indicate that AIBA exhibits some interactions with the negatively charged silica surface owing to electrostatic attraction between the cationic charges derived from the amidinium groups of AIBA and the anionic dissociated silanol groups of the silica surface. The amount of AIBA adsorbed was found to be around 2 mg/g silica (Table 3).

TEM analysis

In order to check whether some polymer was formed on the silica surface or not, the latexes were characterized by TEM. Typical TEM micrographs are shown in Fig. 3. The TEM micrograph of bare silica particles is reported in Fig. 3a for comparison, while Fig. 3b and c correspond to nanocomposite particles obtained using

Table 3 Initiators adsorption on the silica surface. The silica concentration was kept at 10 g/l. The contact time was only 5 min

Initiators	Azobis (isobutyronitrile)	Potassium persulfate	2,2′-Azobis(2-amidinopropane) dihydrochloride
Initial concentration (g/l)	0.12	0.12	0.12
Free concentration (g/l)[a]	0.12	0.12	0.1
Amount adsorbed (mg/g silica)	0	0	2

[a] Determined by UV or elemental analysis of the serum after separation of adsorbed initiator

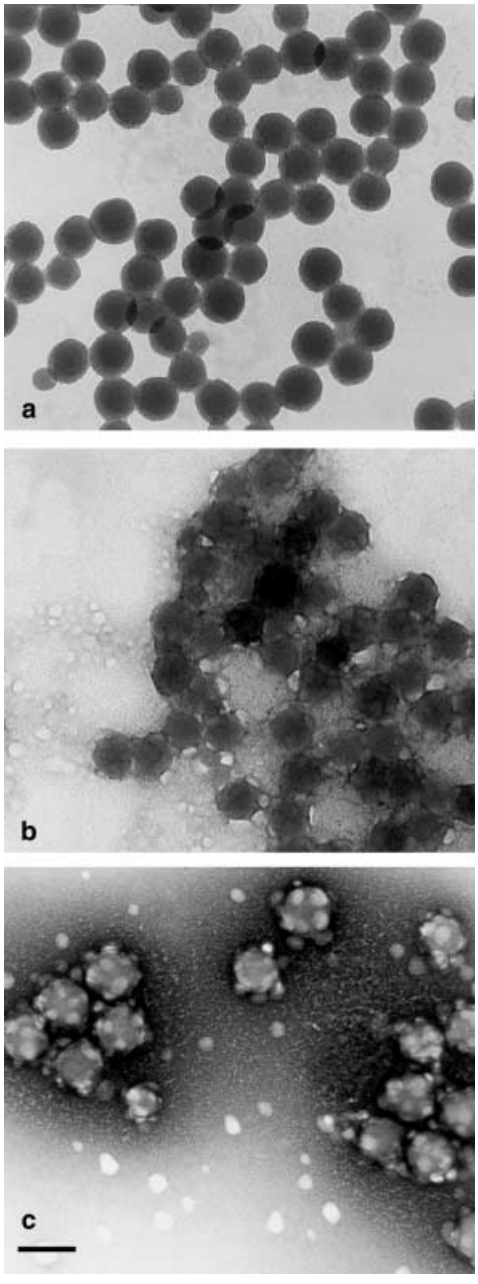

Fig. 3 Transmission electron microscope micrographs of **a** bare silica particles and silica–poly(methyl methacrylate) composite particles synthesized in the presence of **b** 2,2′-azobis(2-amidinopropane) dihydrochloride (*AIBA*) and **c** potassium persulfate (*KPS*). *Scale bar*: 100 nm

AIBA and KPS as initiators, respectively. The images in Fig. 3b and c show nanocomposite latexes with a rough surface due to the presence of small PMMA beads surrounding the inorganic seed particles. Free PMMA latex particles can also be detected in addition to coated silica. Similar results were obtained for AIBN; however, the size of the PMMA particles was so small in that case that the TEM micrograph could not be presented for publication.

Efficiency of the coating reaction and polymer content of the composite particles

The efficiency of the coating reaction and the polymer content of the composite particles were evaluated by extracting the free polymer and analyzing the residue as described in the experimental part. Typical thermogravimetric/differential thermogravimetric analysis (DTG) curves of the composite sample are given in Fig. 4. The DTG curve in Fig. 4 reveals two principal thermal events occurring in the following temperature ranges: 25–200 and 200–700 °C. The first zone can be attributed to the desorption of water and initiator fragments, while the second weight loss corresponds to the PMMA or NP_{30} decomposition. Since the two compounds decompose at almost the same temperature, it was not possible to discriminate between PMMA and NP_{30} by thermogravimetric analysis. Similarly, only the total PMMA and NP_{30} concentration could be estimated by elemental analysis since the carbon might come from both the NP_{30} and the PMMA (see Appendix). Therefore, only the overall (PMMA and NP_{30}) concentration could be calculated at this stage. The results are reported in Table 4 for the three latexes of the series. The results in Table 4 indicate that the weight loss determined by thermogravimetric analysis is in good agreement with the total (PMMA and NP_{30}) concentration determined by elemental analysis. In order to know exactly the amount of silica, PMMA and NP_{30} in both the composite and the free polymer samples, it was decided to perform a quantitative analysis using a material balance.

Material balance

The material balance was performed on a known amount of latex containing known quantities of silica, polymer and surfactant. After quantitative separation of the free latex particles, the amount of composite and free polymer was determined gravimetrically. We found a good balance between the total amount of solid contained in the latex sample and the total amount of recovered products. The silica and (PMMA and NP_{30}) concentrations of the composite and free polymer samples were determined from their carbon and silicon contents, respectively, as described in the Appendix (Table 5). From these data and the amount of recovered product, the quantities of silica and (PMMA and NP_{30}) in the residue and the serum samples could be determined precisely and compared to the theoretical values (Table 6). The PMMA and NP_{30} contents were evaluated separately from the NP_{30}-to-PMMA weight ratio

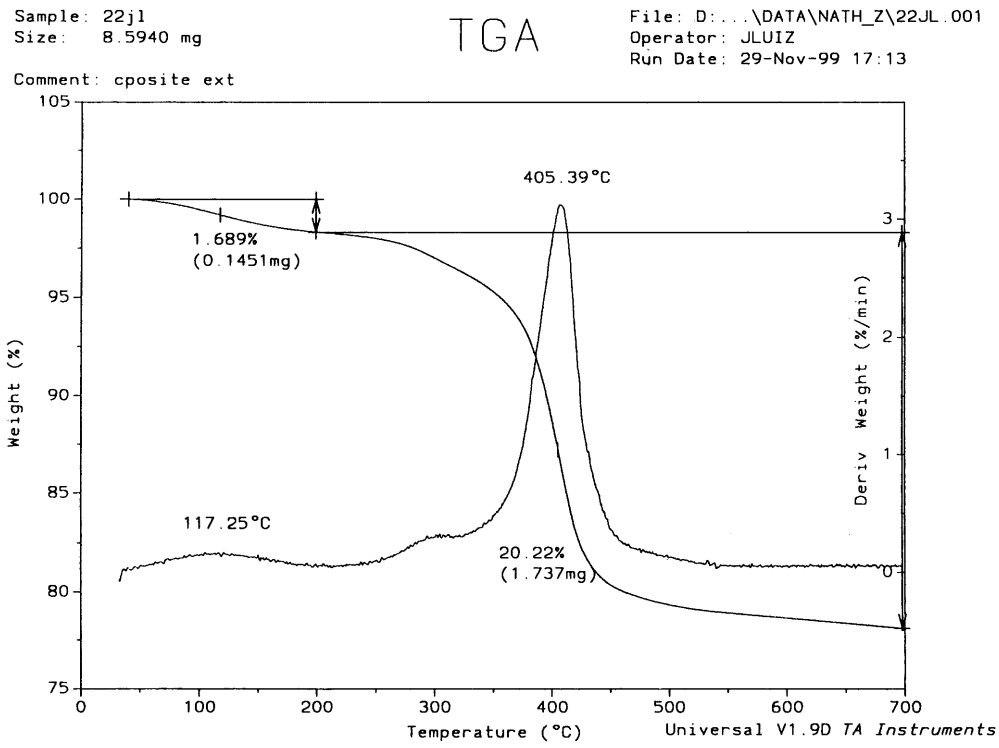

Fig. 4 Thermogravimetric analysis of the composite sample JL22

determined by ^{1}H NMR analysis of the serum sample (see Appendix). The amount of NP_{30} in the residue was then obtained by the difference in the weight between the total amount and the amount of NP_{30} in the serum, while the amount of PMMA was calculated from (PMMA and NP_{30}) by subtracting the amount of NP_{30}. The data reported in Table 6 indicate good agreement between the experimental results and the theoretical values.

The results in Table 6 show that although the surfactant, NP_{30}, was present at a high concentration, it could be quantitatively extracted from the surface of the silica/PMMA nanocomposite particles (no residual NP_{30} was found in the residue). In addition, we show that the composite particles were also selectively separated from the free PMMA latex particles since nearly no silica was found in the serum under our experimental conditions. Consequently, from the data in Table 6, one can determine with precision the efficiency of the coating reaction and the polymer content as described in the experimental part. The results are reported in Table 7 and illustrated in Figure 5. Since no residual surfactant is adsorbed at the surface of the composite particles after extraction, the polymer content of the composite sample and the coating efficiency can also be determined directly from the thermogravimetric analysis data (Table 4). The two sets of values are reported in Table 7 along with the

Table 4 Elemental and thermogravimetric analyses of the composite samples

Samples	Elemental analysis (wt%)		Thermogravimetric analysis (wt%)	
	C	PMMA + NP_{30}	H_2O[a]	PMMA + NP_{30}[b]
JL9	20.6	34.6	1.5	34.9
JL22	12.3	20.7	1.9	20.2
JL148	3.5	5.9	1.64	6.2

[a] Determined from the weight loss between 25 and 200 °C
[b] Determined from the weight loss between 200 and 700 °C

Table 5 Chemical analyses of the composite and the free polymer samples

Samples Content (wt%)	JL9		JL22		JL148	
	Composite	Free polymer	Composite	Free polymer	Composite	Free polymer
Si	29.9	1.7	35.9	0.6	42.4	0.9
C	20.6	54	12.3	54.8	3.5	56.2
SiO_2	62.9	3.6	75.5	1.3	89.2	1.9
PMMA + NP_{30}	34.6	90.7	20.7	92.1	5.9	94.4

Table 6 Material balance

Sample composition	PD9				PD22				PD148			
	Residue	Serum	Total	Theoretical	Residue	Serum	Total	Theoretical	Residue	Serum	Total	Theoretical
SiO_2 (g)	0.088	0.003	0.091	0.094	0.103	0.00155	0.1045	0.117	0.33	0.006	0.336	0.3481
PMMA + NP_{30} (g)	0.048	0.082	0.13	0.138	0.028	0.109	0.137	0.14	0.022	0.29	0.312	0.334
PMMA (g)	0.044	0.024[a]	0.068	0.076	0.028	0.042[a]	0.07	0.08	0.022	0.066[a]	0.088	0.117
NP_{30} (g)	0.004	0.058[a]	0.062	0.062	0	0.067[a]	0.067	0.06	0	0.224[a]	0.224	0.217

[a] Determined knowing the weight ratio, *A*, of NP_{30} over PMMA (see the text)

Table 7 Efficiency of the coating reaction, polymer content and nonextractable polymer content of the composite product

Method	Initiator	2,2′-Azobis (2-amidinopropane) dihydrochloride	Potassium persulfate	Azobis (isobutyro-nitrile)
Material balance	Coating efficiency (wt%)[a]	64.7	40	25
	Polymer content (wt%)[b]	32.3	21.4	6.25
Thermogravimetric analysis	Coating efficiency (wt%)[a]	66.3	37.0	19.6
	Polymer content (wt%)[b]	34.9	20.2	6.2
	Nonextractable polymer content (wt%)[c]	10.0	8.2	3.7
	Nonextractable polymer (mg/g silica)	110	89	38

[a] Percent by weight of the total amount of PMMA synthesized
[b] In weight percent of the composite sample
[c] In weight percent of the amount of recovered product after extraction in toluene

nonextractable polymer content of the composite sample. The data obtained by the two techniques are in good agreement and definitely attest for the validity of the method used for the determination of both the efficiency of the coating reaction and the polymer content of the composite particles under our experimental conditions.

The results reported in Fig. 5 clearly indicate that a high coating efficiency and a high polymer content were obtained when AIBA was used as the initiator. As much as 65% by weight of the total amount of polymer synthesized was found to cover the silica surface when the polymerization reaction was initiated by AIBA, while only 40 and 25% were found to be surface polymer when the anionic and the nonionic initiators were used, respectively. In addition, a higher amount of nonextractable polymer was also obtained when AIBA was used as the initiator in comparison to the anionic or the nonionic initiators (Table 7).

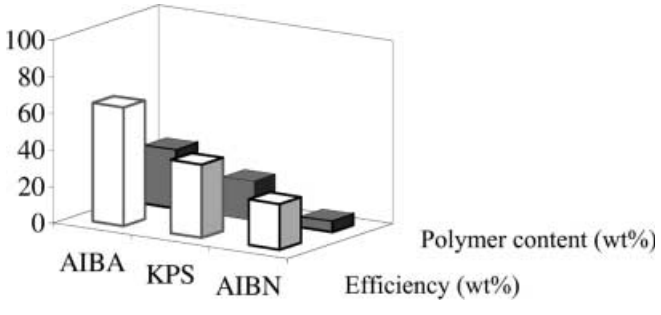

Fig. 5 Coating efficiency and polymer content (determined by elemental analysis) of the composite particles as a function of the type of initiator, AIBA, KPS, azobis(isobutyronitrile), *AIBN*, used in the polymerization reaction

Characterization of the composite latexes

Polymer molecular weight and molecular weight distributions

The polymer molecular weight and the molecular weight distribution of the free latex particles and the extractable coating polymer are reported in Table 8 for the three samples of the series.

The molecular weights of the coating and the free polymers are very similar, while the polymolecularity of

Table 8 Molecular weight and molecular weight distribution of the free polymer and the extractable coating polymer

Samples	Free polymer			Extractable coating polymer[a]		
	M_n	M_w	*I*	M_n	M_w	*I*
JL9	249,000	464,000	1.9	220,000	489,000	2.2
JL22	360,000	632,000	1.7	370,000	664,000	1.8
JL148	319,000	593,000	1.9	260,000	702,000	2.7

[a] Polymer extracted from the composite sample by refluxing in toluene

the coating polymer is higher than that of the free polymer for samples JL9 and JL148.

IR spectroscopy

The composite sample was characterized by IR spectroscopy (Fig. 6). The spectrum in Fig. 6 supports the view that the composite particles are composed of silica and PMMA with the presence of vibration absorption bands characteristic of silica at 1087 cm^{-1} (υ Si–O–Si) and 799 cm^{-1} (δ O–H) and bands at 1735 cm^{-1} (υ C=O), 2947 cm^{-1} (υ CH_2) and 3001 cm^{-1} (υ CH_3) corresponding to PMMA. The assignments are reported in the figure. IR analysis also confirms the absence of the nonionic surfactant in the composite sample.

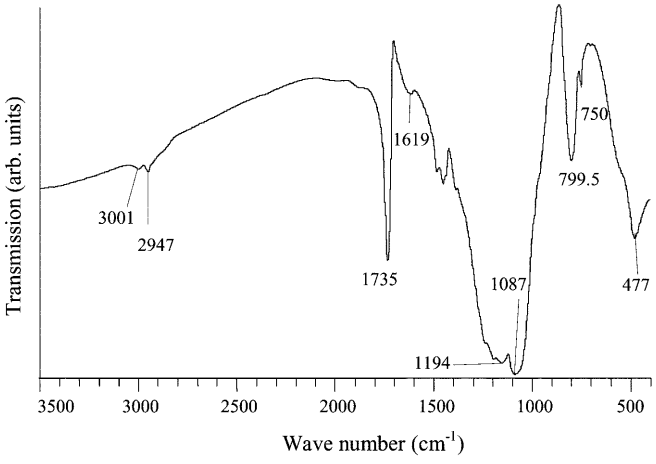

Fig. 6 IR spectrum of the composite sample after separation of the free latex particles

Diameter of the composite latex particles

Though all the latexes are stable to the eye, the TEM micrograph in Fig. 3b shows silica beads glued together as small strings or larger aggregates when AIBA is used as the initiator. Although it is difficult to determine whether aggregation took place on drying or if it is representative of particles clusters formed in the aqueous suspension, it is worthwhile to notice that the diameter of the composite latex particles determined by DLS, i.e., 239 nm, is significantly larger than the diameter they should have if all the polymer formed a regular shell around silica (i.e., 94 nm). Therefore, it can be concluded that the composite latex particles synthesized in presence of AIBA are composed of small aggregates in agreement with the TEM observation. The same conclusion can be reached for AIBN, whereas DLS measurements indicate that the diameter of the composite particles is very close to the theoretical one (i.e., 91 nm) when KPS is used as the initiator.

Discussion

Since colloidal silica carries negative charges under alkaline conditions, as attested by zeta potential measurements (Table 1), electrostatic attractions are likely to take place between the silica surface and the cationic amidinium groups of the diazo compound when AIBA is used as the initiator. Therefore, AIBA is expected to adsorb on silica and to initiate the surface polymerization of methyl methacrylate as represented in Scheme 1.

The adsorption of AIBA on colloidal silica is clearly evidenced by UV analysis of free AIBA in solution (Table 3), while the formation of PMMA on the silica surface is shown in the TEM micrograph in Fig. 3b and

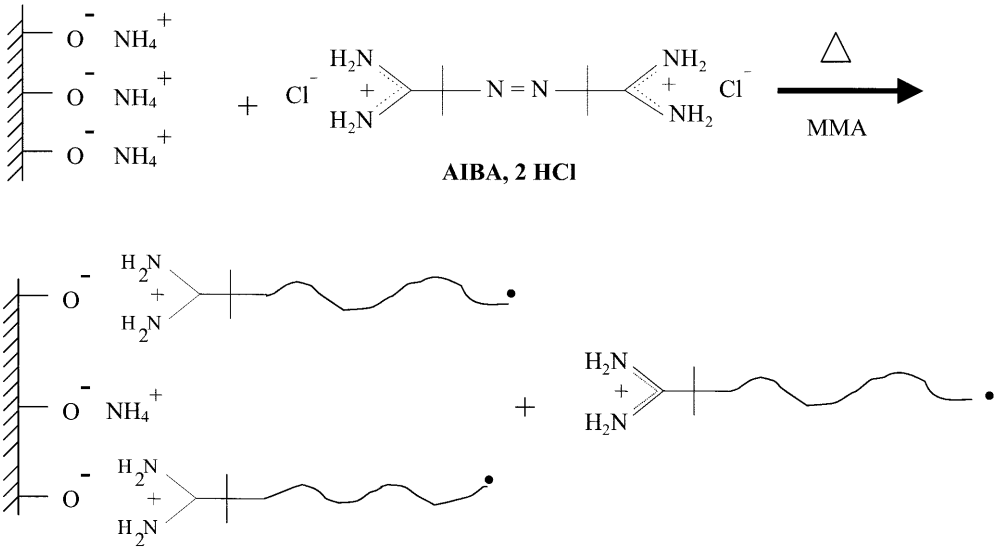

Scheme 1 Schematic representation of the polymerization reaction of methyl methacrylate (*MMA*) initiated by 2,2′-azobis(2-amidinopropane) dihydrochloride (*AIBA*) adsorbed on colloidal silica

is supported by IR spectroscopy analysis of the composite product (Fig. 6). In addition to the formation of surface polymer, the image in Fig. 3b also reveals the presence of free polymer particles resulting from initiation and propagation reactions in the continuous phase. Indeed, in our system, the initiator molecules solubilized in water and the initiator fragment which escapes the silica surface upon thermal decomposition can initiate the polymerization reaction of methyl methacrylate and give cationic latex particles. These primary latex particles can adsorb surfactant and become stable mature particles but they can also be attracted in the course of the reaction by the silica surface and heterocoagulate on the seed mineral as depicted in Fig. 7.

This in situ heterocoagulation mechanism is qualitatively supported by the TEM micrograph in Fig. 3b, which shows many polymer spots deposited on the silica surface and is in agreement with quantitative analysis which demonstrates that 65% by weight of PMMA is obtained as surface polymer while 25 wt% of PMMA remains suspended in the aqueous phase in the form of free latex particles. Such electrostatic effects are widely described in the literature. They have been observed, for instance, during the encapsulation reaction of titanium dioxide pigments [17] and graphite [23] with PMMA. When the charge of the inorganic surface is opposite to that of the growing radicals, attractions can take place in the early stage of polymerization and polymer is formed on the mineral surface in high yield [21]. Because strong electrostatic interactions take place, it can be expected that part of the polymer formed strongly adheres to the mineral surface. In the present experiments, we demonstrate that 20% by weight of the total amount of coating polymer is tightly bound to silica and cannot be extracted with toluene. Moreover, the fact that the molecular weight distribution of the coating polymer is higher than that of the free latex particles (Table 8) supports the idea that the silica particles actively participate in the formation of surface polymer. So, all the results indicate that AIBA plays a determining role in the coating reaction of colloidal silica through emulsion polymerization promoting the formation of polymer on the seed mineral presumably by means of electrostatic interactions, although the occurrence of polymer bonding by means of effects other than charge attractions, for instance, transfer or termination reactions occurring on active sites formed on silica, cannot be discarded at the present time.

Considering now the anionic or the nonionic initiators, the results in Table 3 demonstrate that in agreement with their chemical structures (scheme 2), they do not interact with the silica surface under our experimental conditions. Surprisingly, however, when AIBA is replaced by KPS or AIBN, TEM analysis still reveals the formation of nanocomposite particles with a strawberry-like morphology characterized by small latex beads deposited on the silica surface. Obviously, we must consider that parameters other than the simple surface charges interactions influence the coating mechanism in the present case. Indeed, it is well known that surfactants also play a determining role in coating reactions by increasing the accessibility of the monomer and the growing radicals to the inorganic surface and promoting, consequently, the formation of polymer on the seed mineral [24]. In the present work, we used nonionic NP_{30}, which is known to adsorb on silica in the form of surfactant bilayers [25]. Since we used a large surfactant concentration, well above its critical micellar concentration, we can expect to reach maximum adsorption of NP_{30} on the silica surface. This high amount of adsorbed surfactant may promote the subsequent adsorption of monomer and AIBN molecules as well as that of the growing polymer. Coating is then suspected to take place as follows. Uncharged radicals are formed in the continuous phase upon thermal decomposition of AIBN molecules. Initiation and propagation reactions take place in water generating uncharged oligoradicals. The propagating radicals approach the silica surface and enter the hydrophobic interface formed by the adsorbed bilayer of surfactant. Then, polymer particles precipitate on the silica surface as latex particles which are stabilized by the surfactant already present at the silica/water interface. Concurrently, free latex particles are formed in high yield since a large amount of surfactant is also available for stabilization of particles formed in the continuous phase. This is indeed confirmed by quantitative analysis, which shows that far less polymer is formed on the surface of the silica beads than free latex polymer in the water phase.

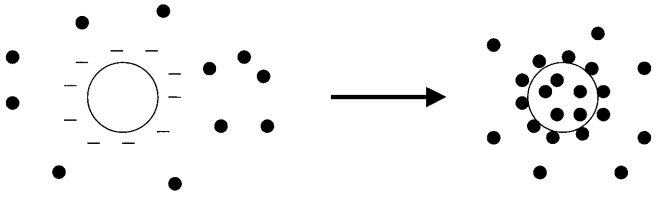

Fig. 7 Schematic representation of the coating reaction of colloidal silica in alkaline medium using AIBA as cationic initiator

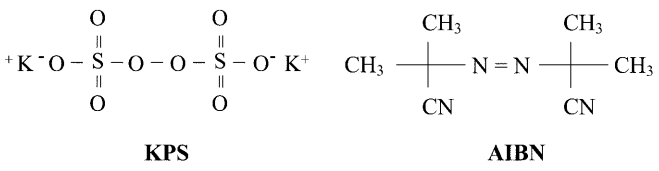

Scheme 2 Chemical structures of potassium persulfate (*KPS*) and azobis(isobutyronitrile) (*AIBN*)

When KPS is used as the initiator, it can be hardly accepted that the radicals formed in water are captured on the inorganic seed surface under our experimental conditions owing to the electrostatic energy barrier between silica and the growing negatively charged polymer chains. Consequently, all the polymer should be formed as free latex particles in that case. However, quantitative analysis shows that the efficiency of the coating reaction and the polymer content are significantly high when KPS is present.

It is well known that the thermal decomposition of the persulfate ions gives sulfate radicals according to

$$S_2O_8^{2-} \rightarrow 2SO_4^{\cdot -}. \quad (4)$$

The $SO_4^{\cdot -}$ radical, however, is considered to be unstable and to hydrolyze in aqueous solutions, giving rise to a hydroxyl radical [26].

$$SO_4^{\cdot -} + H_2O \leftrightarrow OH^{\cdot} + SO_4^{2-} + H^+ \quad (5)$$

Therefore, a possible explanation for the high coating efficiency observed in presence of KPS, is the formation of hydroxyl neutral radicals capable of diffusing into the hydrophobic surfactant bilayer formed on the silica surface and of creating reaction loci as described previously for polymerization reactions initiated with AIBN. Thus, electrostatic repulsions between the electrical double layer at the silica surface and radicals are no longer a problem if one considers that initiation occurs by way of hydroxyl radicals formed by interaction of $SO_4^{\cdot -}$ with water, rather than by the $SO_4^{\cdot -}$ radical ions themselves. However, even if it has been shown that the $SO_4^{\cdot -}$ radical may be converted to $OH^{\cdot}$ radicals in alkaline solutions [27], it is well known that the formation of $OH^{\cdot}$ radicals preferentially takes place in acidic conditions [28]. Consequently, a more plausible assumption, under our experimental conditions, is the formation of $NH_2^{\cdot}$ radicals produced by the oxidative reaction of $OH^{\cdot}$ or $SO_4^{\cdot -}$ radicals with ammonia, which is present in high concentrations in our polymerization medium [29].

$$OH^{\cdot} + NH_3 \rightarrow H_2O + NH_2^{\cdot}, \quad (6)$$

$$SO_4^{\cdot -} + NH_3 \rightarrow SO_4^{2-} + NH_2^{\cdot} + H^+. \quad (7)$$

Obviously, both the hydroxy- and the amino-terminated species described previously should have a higher tendency to adsorb on silica, by, for instance hydrogen bonding, than ionized sulfate-terminated species. However, in comparison to the alkyl radicals produced by thermal dissociation of AIBN, the fact that $OH^{\cdot}$ or $NH_2^{\cdot}$ radicals give a better coating efficiency than the radicals produced upon decomposition of AIBN is not straightforward. To account for this result, one must assume that the $SO_4^{\cdot -}$ or $OH^{\cdot}$ radicals can also react with ammonium ions in the electrical double layer as follows:

$$NH_4^+ + SO_4^{\cdot -} \rightarrow HSO_4^- + NH_3^{\cdot +}, \quad (8)$$

$$OH^{\cdot} + NH_4^+ \rightarrow H_2O + NH_3^{\cdot +}. \quad (9)$$

The $NH_3^{\cdot +}$ radical formed in the double layer is then expected to adsorb on silica and may explain the high coating efficiency observed when KPS is present by analogy to what was described previously when a cationic molecule is used as the initiator. This explanation is supported by the TEM observations, which show that the nanocomposites synthesized in the presence of KPS and AIBA have similar morphologies, suggesting that they were obtained by similar mechanisms. Another possibility that must be considered is the reaction by hydrogen-atom abstraction of the sulfate radicals and, more probably, the $OH^{\cdot}$ or the $NH_2^{\cdot}$ radicals with the silanol groups of the silica surface according to

$$SiOH + OH^{\cdot} \rightarrow SiO^{\cdot} + H_2O, \quad (10)$$

$$SiOH + NH_2^{\cdot} \rightarrow SiO^{\cdot} + NH_3. \quad (11)$$

Although, we do not have any evidence of it, the formation of free radicals directly attached to the silica surface could surely explain the high coating efficiency obtained when KPS is present. Indeed, one can assume that the polymer chains immobilized at the silica surface at the very beginning of the reaction could catch radicals and become active sites for the nucleation and growth of polymer particles. In addition, the formation of $SiO^{\cdot}$ free radicals on the silica surface may be also responsible for the large amount of bonded polymer formed when KPS is used as the initiator (Table 7).

Conclusions

Silica/PMMA nanocomposite latex particles were synthesized in emulsion polymerization using either a cationic, an anionic or a nonionic initiator. At the end of the reaction, the composite particles were separated from the free polymer phase using a series of centrifugations/redispersions in water. The polymer content of the composite samples and the efficiency of the coating reaction were determined by thermogravimetric analysis and the results were confirmed by a material balance. We found that the polymer content and the coating efficiency depend greatly on the nature of the initiator. The best results are obtained for the cationic initiator: AIBA. AIBA adsorbs on silica and can initiate polymerization reactions on its surface; however, AIBA can also initiate polymerization in the continuous phase and generate positively charged latex particles which can adsorb, in situ, on the silica surface giving nanocomposite particles with a strawberry-like morphology. Heterocoagulation, which involves electrostatic attrac-

tion between the inorganic particles and the cationic polymer, seems to be, in that case, the driving force of the coating reaction. Though electrostatic attraction are unlikely to take place when KPS or AIBN are used as initiators, PMMA deposition on the silica surface in the form of small polymer beads has also been evidenced for these two compounds. Whilst the polymer chains initiated by AIBN can approach the silica surface and develop interactions with the surface silanol groups or with the adsorbed surfactant by hydrogen bonding, such a mechanism seems unlikely to take place in the case of KPS owing to the repulsion forces existing between the anionic radicals and the negatively charged silica surface. Therefore, the reason why surface polymer is formed in high yield when KPS is used as initiator is presumably the possibility to generate $OH^{\cdot}$ or $NH_2^{\cdot}$ free radicals which can abstract hydrogen on the silanol groups. These attached radicals can also explain the large amount of bonded polymer obtained when KPS is present. Another possibility is the formation of $NH_3^{\cdot+}$ radicals in the double layer attracted in situ by the silica surface.

It is clear that further work should be done to clarify the mechanism leading to the formation of nanocomposite particles when KPS or AIBN are used as initiators. However, we have decided rather to bring more attention to AIBA, which appears to be the best initiator of the series. Publications are presently in preparation to describe in more depth the mechanism of heterocoagulation and the fundamental aspects associated with the use of a cationic initiator in the synthesis of silica/PMMA nanocomposite latex particles through emulsion polymerization.

Acknowledgements The authors thank Roger Spitz for financially supporting this work and Christian Novat for great help with the TEM images.

Appendix

Determination of the silica, PMMA and NP_{30} concentrations from elemental analysis

The silica concentration was determined as follows:

$$SiO_2(wt\%) = \frac{Si(wt\%) \times 61}{29}, \quad (A1)$$

where 29 and 61 correspond to the Si and SiO_2 molecular weights, respectively.

The PMMA and NP_{30} concentrations were calculated according to Eqs. (A2) and (A3):

$$PMMA(wt\%) = \frac{C(wt\%) \times 100}{5 \times 12} = 1.66 \times C(wt\%), \quad (A2)$$

$$NP_{30}(wt\%) = \frac{C(wt\%) \times 1540}{75 \times 12} = 1.71 \times C(wt\%), \quad (A3)$$

where 100 and 1540 are the methyl methacrylate and NP_{30} molecular weights, and 5 and 75 are the total number of carbon atoms per molecule. Considering that Eqs. (A2) and (A3) are very similar, the overall PMMA plus NP_{30} concentration can be satisfactorily estimated by

$$PMMA + NP_{30}(wt\%) \approx 1.68 \times C(wt\%). \quad (A4)$$

Determination of the NP_{30}-to-PMMA weight ratio by ^1H NMR analysis

The molar ratio of ethylene oxide units to methyl methacrylate was determined by ^1H NMR analysis as

$$NP_{30}/PMMA(mole/mole) = 2a/4b, \quad (A5)$$

where a is the area of the peak resonance at 6.5–7.5 ppm corresponding to the aromatic protons (C_6H_4) of NP_{30} and b is that of the methylene protons of PMMA (CH_2: 1.8–2.1 ppm). The weight ratio, A, of NP_{30} to PMMA is given by

$$\begin{aligned} A &= NP_{30}/PMMA(g/g) \\ &= NP_{30}/PMMA(mol/mol)(1540/100). \end{aligned} \quad (A6)$$

Knowing $x = PMMA + NP_{30}$ and the weight ratio, A, of NP_{30} over PMMA, one can find

$$PMMA = \frac{x}{A+1} \quad \text{and} \quad NP_{30} = \frac{Ax}{A+1}. \quad (A7)$$

References

1. Li X, Sun Z (1995) J Appl Polym Sci 58:1991
2. Lee J, Senna M (1995) Colloid Polym Sci 273:76
3. Ozin GA (1992) Adv Mater 4:612
4. van Herk AM, German AL (1999) In: Arshady R (ed) Microspheres microcapsules and liposomes, vol 1. Preparation and chemical applications. Citus, London, pp 457 f
5. Caris CHM, van Elven LPM, van Herk AM, German AL (1989) Br Polym J 21:133
6. Templeton-Knight RL (1990) J Oil Colour Chem Assoc 73:459
7. Templeton-Knight RL (1990) Chem Ind 16:512
8. Zirkzee HF (1997) PhD thesis. Eindhoven, University of Technology, The Netherlands

9. Bourgeat-Lami E, Espiard P, Guyot A, Gauthier C, David L, Vigier G (1996) Angew Makromol Chem 242:105
10. Caris CHM, van Herk AM, German AL (1990) 20th FATIPEC Conference Proceedings. EREC, Puteaux, France, p 325
11. Espiard P, Revillon A, Guyot A, Mark JE (1992) In: Daniels ES, Sudol T, El Aasser M (eds) Polymer latexes: preparation, characterization and applications. ACS Symposium Series 492. American Chemical Society, Washington, DC, p 393
12. Caris CHM (1995) PhD thesis. Eindhoven, University of Technology, The Netherlands
13. Du H, Zhang P, Liu S, Wang D, Li T, Tang X (1997) Polym Int 43:274
14. Janssen RQF, van Herk AM, German AL (1993) J Oil Colour Chem Assoc 11:455
15. Hergeth WD, Starre P, Schmutzler K, Wartewig S (1988) Polymer 29:1323
16. Hergeth WD, Steinau UJ, Bittrich HJ, Simon G, Schmutzler K (1989) Polymer 30:254
17. Haga Y, Watanabe T, Yosomiya R (1991) Angew Makromol Chem 189:23
18. Dekking HGG (1967) J Appl Polym Sci 11:23
19. Dekking HGG (1965) J Appl Polym Sci 9:1641
20. Meier LP, Shelden RA, Caseri WR, Suter UW (1994) Macromolecules 27:137
21. Yoshinaga K, Yokoyama T, Sugawa Y, Karakawa H, Enomoto N, Nishida H, Komatzu M (1992) Polym Bull 28:663
22. Janssen RQF, van Herk AM, German AL (1994) 22nd FATIPEC Conference Book, vol 1. Hungarian Chemical Society, pp 104–118
23. Yamaguchi T, Ono T, Saito Y, Ohara S (1976) Angew Makromol Chem 53:65
24. Hasegawa M, Arai K, Saito S (1987) J Polym Sci 25:3231
25. Rutland MW, Senden TJ (1993) Langmuir 412
26. Bartlett PD, Nozaki K (1948) J Polym Sci 3:216
27. Dogliotti L, Hayon E (1967) J Phys Chem 71:2511
28. Blackley DC (1975) In: Blackley DC (ed) Emulsion polymerization. Applied Science, London, pp 156, 390
29. Alfassi ZB, Huie RE, Neta P (1998) In: Alfassi ZB (ed) The chemistry of free radicals, N-centered radicals. Wiley, New York, pp 515